An energetic Profile of *Corynebacterium glutamicum* underpinned by measured biomass yield on ATP

E. Zelle, N. Pfelzer, M. Oldiges*, A. Koch-Koerfges, M. Bott, K. Nöh, W. Wiechert**

Institute of Bio- and Geosciences, IBG-1: Biotechnology, Forschungszentrum Jülich GmbH, D-52425 Jülich, Germany

** RWTH Aachen University, Institute of Biotechnology, Aachen, Germany*

***RWTH Aachen, Computational Systems Biotechnology, Aachen, Germany*

Email: e.zelle@fz-juelich.de

Abstract

The supply and usage of energetic cofactors in metabolism is a central concern for systems metabolic engineering, particularly in case of energy intensive products. One of the most important parameters for systems wide balancing of energetic cofactors is the ATP requirement for biomass formation $Y_{ATP/Biomass}$. Despite its fundamental importance, $Y_{ATP/Biomass}$ values for non-fermentative organisms are still rough estimates deduced from theoretical considerations. For the first time, we present an approach for the experimental determination of $Y_{ATP/Biomass}$ using comparative ^{13}C metabolic flux analysis (^{13}C MFA) of a wild type strain and an ATP synthase knockout mutant. We show that the energetic profile of a cell can then be deduced from a genome wide stoichiometric model and experimental maintenance data. Particularly, the contributions of substrate level phosphorylation (SLP) and electron transport phosphorylation (ETP) to ATP generation become available which enables the overall energetic efficiency of a cell to be characterized. As a model organism, the industrial platform organism *Corynebacterium glutamicum* is used. *C. glutamicum* uses a respiratory type of energy metabolism, implying that ATP can be synthesized either by SLP or by ETP with the membrane-bound F_1F_O-ATP synthase using the proton motive force (pmf) as driving force. The presence of two terminal oxidases, which differ in their

^{13}C MFA, 13C metabolix flux analysis; CLE, carbon labeling experiment; COBRA, constraint-based reconstruction analysis; D, dilution rate; EMP, Embden-Meyerhof pathway (glycolysis); ETP, electron transport phosphorylation; FBA, flux balance analysis; GAM, growth associated maintenance; Glc0, unlabeled glucose; Glc1, glucose labeled at first position; GlcU, fully-labeled glucose; GLPK, GNU (Betriebssystem) Linear Programming Kit; GUR, glucose uptake rate; HPLC, high performance liquid chromatography; LC-ESI-MS/MS, Liquid chromatography - Electrospray ionization - mass spectrometry; LP, linear programming; MKH2, reduced menaquinone; MS, mass spectrometry; NGAM, non-growth associated maintenance; PFR, plug flow reactor; pmf, proton motive force; P/O ratio, phosphate/oxygen ratio; PPP, pentose phosphate pathway; SLP, substrate level phosphorylation; TCA, citric acid cycle (or tricarboxylic acid); UPT, uptake; WT, wild type

proton translocation efficiency by a factor of three, further complicates energy balancing for this organism. By integration of experimental data and network models, we show that in the wild type SLP and ETP contribute equally to ATP generation. Thus, the role of ETP in respiring bacteria may have been overrated in the past. Remarkably, in the genome wide setting 65% of the pmf is actually not used for ATP synthesis. However, it turns out that, compared to other organisms *C. glutamicum* still uses its energy budget rather efficiently.

Keywords

- ATP yield
- metabolic flux analysis
- constraint based methods
- energy metabolism
- branched respiratory chain

Glossary

The **maximal theoretical ATP yield**, derived from traditional biochemistry knowledge, represents a best-case result based on complete oxidation of one mole of glucose. This value could only be reached under non-growth conditions, using glucose exclusively for ATP synthesis and assuming that no energy losses occur.

Under growth conditions, anabolism requires glucose as well, which has a big influence on the *in vivo* ATP yield (i.e. moles ATP effectively produced per mol glucose uptake). The **maximal *in vivo* ATP yield** represents the physiological potential reached when all reducing equivalents (NADH and MQH_2) supplied by the central carbon metabolism (determined based on the fluxome for growing cells) are converted to ATP.

In contrast, the **effective *in vivo* ATP yield** (of the wild type) is based on the proton needs of the ATP synthase, as calculated based on the fluxome gained by ^{13}C-MFA in combination with $Y_{ATP/Biomass}$. Hence, the maximal *in vivo* ATP yield limits the range for

the effective *in vivo* ATP yield, i.e. the supplied reducing equivalents enable a higher proton translocation than required for growth.

1. Introduction

Depending on the carbon source, aerobic respiring bacteria gain ATP both by substrate level phosphorylation (SLP) and by electron transport phosphorylation (ETP). Together, these two processes for ATP supply govern the energetic housekeeping of the living cell. SLP and ETP are investigated here under aerobic *in vivo* conditions for the non-pathogenic Gram-positive soil bacterium *Corynebacterium glutamicum* [1]. This species is subject to intensive studies as it is a platform organism for large scale biotechnological production of millions of tons of amino acids every year and a still broadening spectrum of other products [2, 3]. Furthermore, *C. glutamicum* serves as a model organism for the order *Corynebacteriales*, which includes a number of important pathogens, e.g. *Mycobacterium tuberculosis*.

As many bacteria, *C. glutamicum* possesses a branched respiratory chain, with at least six different dehydrogenases that transfer electrons to menaquinone (without translocating protons), and can use either oxygen or nitrate as terminal electron acceptor [4] (Figure 1). It is important to note that the composition of the respiratory chain differs from that in mitochondria in that the proton-translocating complex I (NADH dehydrogenase) is missing. Furthermore, due to the use of menaquinone instead of ubiquinone as respiratory quinone, the succinate dehydrogenase reaction is presumably coupled to the import of two protons [5]. Therefore, mitochondria have an energetically higher potential than bacteria. Under aerobic conditions the electrons are passed to oxygen either by the cytochrome bc_1-aa_3 supercomplex or the cytochrome *bd* oxidase [4]. Importantly, the two terminal oxidases differ in their energetic efficiency with respect to proton translocation and oxygen affinity. The efficiency of the

cytochrome bc_1-aa_3 supercomplex is $6H^+/2e^-$, while the cytochrome *bd* oxidase translocates only $2H^+/2e^-$ [6, 7]. The resulting proton motive force (pmf) is the driving force for ATP synthesis by the membrane-bound F_1F_O-ATP synthase. Starting point for the formation of the pmf are the reducing equivalents (NADH and reduced menaquinone – MKH2), generated by the central carbon metabolism. The pmf is built up when the corresponding electrons are passed through the electron transport chain.

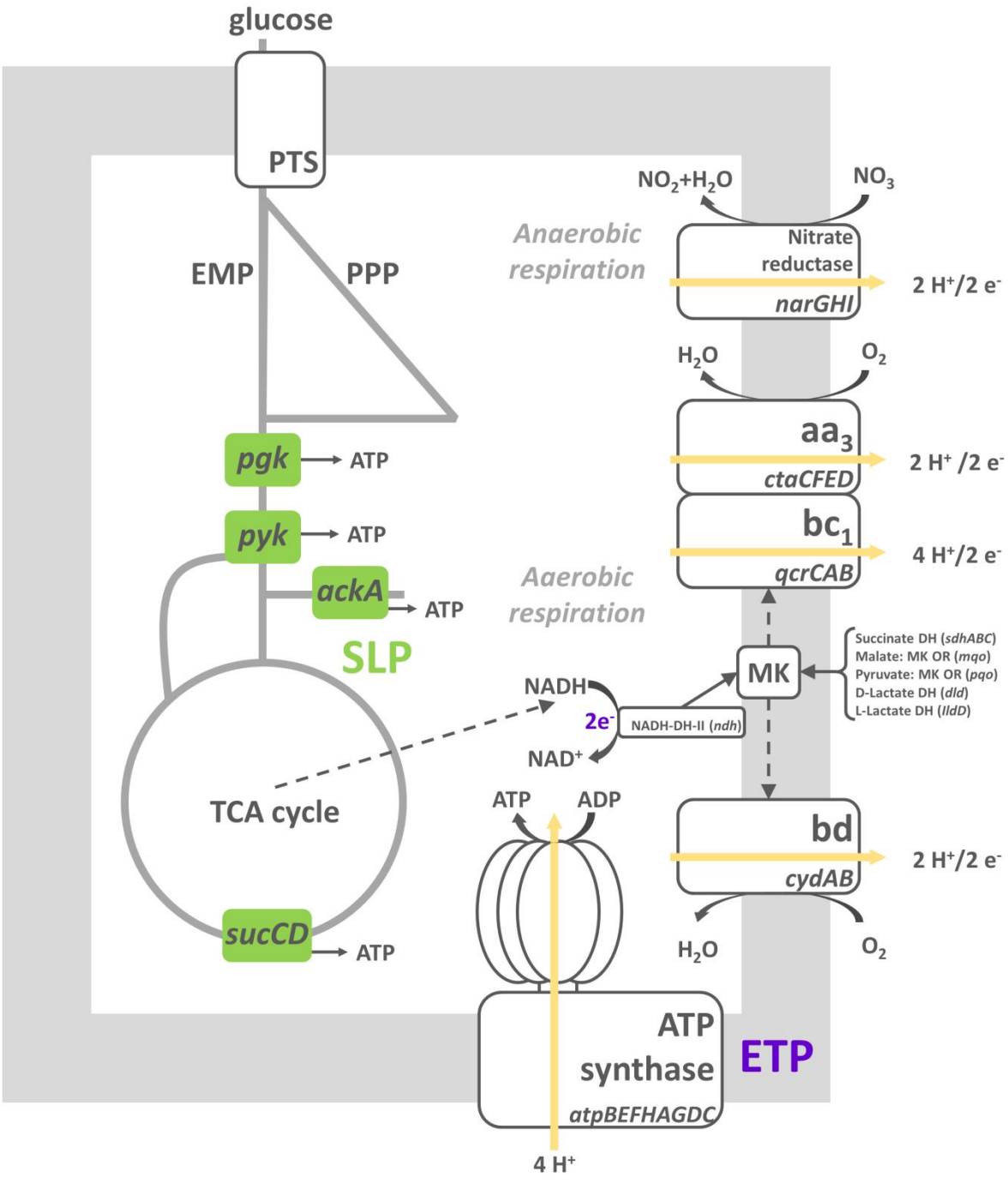

Figure 1: Overview on the components constituting the (aerobic and anerobic) respiratory chain of C. glutamicum. C. glutamicum possesses a branched respiratory chain with at least six different dehydrogenases as well as two terminal oxidases (bd and aa_3).

Figure 1 summarizes all pathways contributing to ATP generation in *C. glutamicum*. While the glucose uptake, glycolysis (Embden-Meyerhof pathway, short: EMP), pentose phosphate pathway (PPP), tricarboxylic acid (TCA) cycle, and anaplerotic reactions are simplified, with just highlighting the SLP reactions, the figure focuses on the components constituting the respiratory chain, i.e. the different dehydrogenases as well as the terminal oxidases. Theoretically, if solely the more efficient bc_1-aa_3 supercomplex is used for generating the pmf, a maximum of 14 ATP could be gained by the ETP (or in total 18 together with 4 ATP from SLP) when one mole of glucose is completely oxidized to CO_2. The P/O ratio then can be calculated as 1.5. Here, according to Bott 2003 [4] the supplied NADPH is not taken into account as the NADPH oxidation by NADH dehydrogenase-II (NDH) is negligible at physiological pH. Furthermore, it must be taken into account that these theoretical values are based on the assumption that the ATP synthase requires 4 H^+ for the formation of one ATP while formally 3 H^+/ATP are assumed [8]. The optimal requirement of 3 H^+/ATP (one per each catalytic site of the ATP synthase) is dodgy and exact number of protons needed for the synthesis of one ATP is still an ongoing issue [9]. Allowing some inefficiency of the proton transfer by ATP synthase makes 4 H^+/ATP more realistic conjecture [10, 11]. In comparison, higher organisms with a mitochondrial electron transport chain can gain up to 32 ATP per glucose molecule (which corresponds to a maximal P/O ratio of 3). Compared to the 18 ATP generated by *C. glutamicum*, bacteria like *P. denitrificans* can render up to 38 ATP and *E. coli* still produces up to 22 (Under physiological conditions, it is not possible to say, which part of glucose is converted to energy, biomass or other products. The reason is that many reaction steps cannot be uniquely

assigned to anabolism or catabolism. Consider, for example, the biomass precursor pyruvate, which generates only the ATP of SLP and the two NADH formed in glycolysis but not the reduction equivalents gained in the TCA cycle nor the ATP formed by succinyl-CoA synthetase. Only in the (theoretical) case of complete usage of glucose for ATP production, this problem does not arise. Under realistic conditions, however organisms have to balance the trade-off between biomass and energy formation. In this situation, effective yield coefficients relating glucose uptake to overall ATP and biomass production are the best way to characterize the catabolic versus anabolic branch.

Table 1). Variations in the respective composition of respiratory chain of these organisms cause the differing ATP yields (with associated P/O ratios). This analysis seems to classify *C. glutamicum* as an organism with low energetic efficiency. However, the calculated (maximal theoretical) ATP yields, derived from traditional biochemistry knowledge, are best-case results. They give the maximal theoretical efficiency of free energy transduction in the energy harvesting machinery of a cell. Reaching these values would only be possible under non-growth conditions, using glucose exclusively for ATP synthesis and assuming that no energy losses occur. Clearly, under growth conditions, anabolism requires glucose as well, which has a big influence on the effective *in vivo* ATP yield (i.e. moles ATP effectively produced per mol glucose uptake under growth conditions).

Under physiological conditions, it is not possible to say, which part of glucose is converted to energy, biomass or other products. The reason is that many reaction steps cannot be uniquely assigned to anabolism or catabolism. Consider, for example, the biomass precursor pyruvate, which generates only the ATP of SLP and the two NADH formed in glycolysis but not the reduction equivalents gained in the TCA cycle

nor the ATP formed by succinyl-CoA synthetase. Only in the (theoretical) case of complete usage of glucose for ATP production, this problem does not arise. Under realistic conditions, however organisms have to balance the trade-off between biomass and energy formation. In this situation, effective yield coefficients relating glucose uptake to overall ATP and biomass production are the best way to characterize the catabolic versus anabolic branch.

*Table 1– theoretical maximal ATP yields: Maximal amount of ATP produced by the oxidation of one mol glucose of plants, mitochondria, and different microbes [12]. The difference between the total ATP yields of the different species is caused by the deviating composition of the ETP. Moreover, it is important to keep in mind that the upper values are based on the assumption that three protons are needed for the synthesis of one ATP, whereas the C. glutamicum values marked with * are based on four H^+ per ATP. Finally, it should be mentioned that all values assume that the pmf is exclusively used for ATP production.*

	SLP	**ETP**	**total ATP**
plants	4 (11.1%)	32 (88.9%)	36
mitochondria	4 (12.5%)	28 (87.5%)	32
P. denitrificans	4 (10.5%)	34 (89.5%)	38
E. coli	4 (15.4%)	22 (84.6%)	26
C. glutamicum bd branch (100%)	4 (42.9%)	5.3 (57.1%)	9.3
C. glutamicum bc_1-aa_3 branch (100%)	4 (17.6%)	18.7 (82.4%)	22.7
C. glutamicum bd branch (100%)*	4 (50.0%)	4 (50.0%)	8
C. glutamicum bc_1-aa_3 branch (100%)*	4 (22.2%)	14 (77.8%)	18

Moreover, there are also several intrinsic energy losses in the oxidative phosphorylation (OxPhos) which strongly influence the effective *in vivo* ATP yield:

1. The ATPase efficiency might be worse than the assumed value of 4 protons per ATP produced, which further decreases the efficiency of the ETP.
2. Translocated protons are not only used for ATP synthesis. They are also involved in pH homeostasis and membrane transport processes. Additionally, a proton leakage to the surrounding medium cannot be excluded.

3. Due to the branched nature of the respiratory chain of *C. glutamicum* (as for the majority of aerob bacteria), the magnitude of the pmf generated per electron can vary. When both the bc_1-aa_3 supercomplex and the *bd* oxidase are active, proton translocation ranges between $2H^+/2e^-$ and $6H^+/2e^-$ corresponding to a range of 4 to 14 ATP produced by ETP per glucose molecule.

In all three cases only the ETP efficiency (14 ATP per glucose at maximum) decreases whereas the 4 ATP generated by SLP remain untouched.

For the following, it is very important to understand, that these 4 ATP are a net value obtained from the ATPs produced and consumed in SLP. *C. glutamicum* takes up glucose via a PTS-system, which is phosphoenolpyuruvate/pyruvate (PEP/PYR), but not ADP/ATP, coupled, Consequently, SLP produces 5 and consumes 1 ATP (for phosphofructokinase) in contrast to the 6 versus 2 usually shown in textbooks for other organisms. Although this leads in both SLP configurations to the net amount of 4 ATP it makes a difference in the context of a whole cell stoichiometric model. Here, the in- and out-fluxes of the global ATP pool will be lower, when only 5 instead of 6 ATPs are generated and only 1 instead of 2 ATPs are withdrawn. This consideration will become important later on, when discussing the efficiency of ATP production.

For example, the effective contribution of SLP to total ATP production is usually given by 4/(4+14)=22% when only the net production of glycolysis is considered. In contrast, in the context of a genome wide stoichiometric model operating with the theoretical maximum ATP yield (i.e. no biomass production), the SLP contribution to total ATP production is 5/(5+14)=26% in *C. glutamicum* and even 6/(6+14)=30% in organisms where glycolysis is fueled by hexokinase. Summarizing, while normally net values are considered for glycolysis, we assume the pure ATP gain without considering the ATP consumption of the pfk (i.e. this is a gross yield).

Even the effect of taking the pentose phosphate pathway (PPP) route instead of (upper) glycolysis, is not that easy to calculate. Then, the SLP yield drops to 3.3 due to the loss of one carbon in the oxidative PPP. However, this carbon loss also reduces the amount of supplied reduction equivalents and thus decreases both SLP and ETP. The combined effect can only be properly analyzed by using a stoichiometric network model (see below). However, the catabolic versus anabolic substrate usage has a much bigger effect on the effective ATP yield, which is under *in vivo* conditions certainly far below the theoretical maximum of 18 for *Corynebacterium*.

Although the given arguments suggest that in *C. glutamicum* the ETP share on total ATP generation might be much lower than the maximum value of 78% (Under physiological conditions, it is not possible to say, which part of glucose is converted to energy, biomass or other products. The reason is that many reaction steps cannot be uniquely assigned to anabolism or catabolism. Consider, for example, the biomass precursor pyruvate, which generates only the ATP of SLP and the two NADH formed in glycolysis but not the reduction equivalents gained in the TCA cycle nor the ATP formed by succinyl-CoA synthetase. Only in the (theoretical) case of complete usage of glucose for ATP production, this problem does not arise. Under realistic conditions, however organisms have to balance the trade-off between biomass and energy formation. In this situation, effective yield coefficients relating glucose uptake to overall ATP and biomass production are the best way to characterize the catabolic versus anabolic branch.

Table 1), it is commonly assumed that under aerobic conditions the ETP still dominates SLP [13, 14]. As suggested in [13], this theoretically motivated assumption probably overestimates the ATP contribution by ETP under physiological conditions. In the

present investigation, this hypothesis is challenged by analyzing ATP generation in a systems-wide context based on experimental data and metabolic modeling.

This investigation is primarily concerned with the determination of ATP requirement for biomass formation ($Y_{ATP/Biomass}$) as an effective yield coefficient. At present state, molar physiological ATP yields (with respect to glucose) for non-fermentatively growing organisms are rarely found in literature and most often based on theoretical considerations only. One approach is to calculate the amount of ATP required for forming cell material from the macromolecular composition by making assumptions e.g. on the amount of ATP required for the incorporation of one mole of amino acids into protein [15, 16]. Other studies are based on the maximal theoretical ATP yields of the complete catabolism of one mole of substrate to CO_2 and ATP, which doubtlessly overestimates the effective *in vivo* ATP formation [17, 18].

The step forward in determination of the effective *in vivo* ATP yield of *C. glutamicum* presented here is that it is derived quantitatively in a two-step approach from experimental data integrated with a network model. To determine $Y_{ATP/Biomass}$ and, in consequence, the share of SLP and ETP on ATP synthesis in growing cells a mutant strain of *C. glutamicum* ATCC 13032 lacking the ATP synthase, henceforth named *C. glutamicum* ΔF_1F_O, was used [13]. This strain can generate ATP solely by SLP.

The ATP synthase knockout mutant lacking the *atpBEFHAGDC* genes encoding the F_1F_O-ATP synthase was described in [13]. Briefly, the characterization of the *C. glutamicum* ΔF_1F_O (conducted in shake-flask cultivations on minimal medium) showed that the mutant reached 47% of the growth rate and 65% of the biomass of the wild type (WT), while no growth on acetate as sole carbon source was observed. The mutant exhibits a bi-phasic growth on glucose as sole carbon source. The first growth phase is characterized by an increased glucose uptake rate, high oxygen

consumption and pyruvate secretion. The second growth phase is initiated by an oxygen limitation and is accompanied by a reduced glucose uptake rate and a resumption of pyruvate. Furthermore, the mutant showed a decreased glycogen accumulation and higher excretion of organic acids. Concluding, the observation that *C. glutamicum* ΔF_1F_O can still grow with a growth rate of 0.19 h^{-1} proves that the ATP synthase is in general not essential for growth of *C. glutamicum* [13].

Due to the fact that *C. glutamicum* ΔF_1F_O solely relies on SLP, all ATP producing reactions are known to be located in the central carbon metabolism. Thus, they are amenable to ^{13}C metabolic flux analysis (^{13}C MFA). Here, the important point is that ^{13}C MFA does not need any assumptions on the usage of energetic cofactors, which makes this technique suited to quantify the contributions of the SLP in an unprejudiced way [19]. In particular, this applies for the reactions that supply the reducing equivalents NADH and MKH2. Hence, for the first time the ATP synthase deficient mutant in combination with ^{13}C MFA may allow for the determination of $Y_{ATP/Biomass}$ [mol/g_{CDW}] without making any further assumptions concerning the energy needs. Notably, the network structure automatically takes into account a proportionately usage of the glucose for biomass and energy.

Once having calculated $Y_{ATP/Biomass}$, this value enables to derive the full energetic profile of *C. glutamicum* including the detailed contributions of all ATP producing reactions. Particularly, the question how much of the pmf is used for ATP synthesis can be answered. Clearly, the branched electron transfer chain of *C. glutamicum* is complicating the analysis of energetic efficiency. We show that by putting the ^{13}C MFA findings obtained from a central metabolic network model into the larger picture of a genome wide network of *C. glutamicum* [20], more insight into the usage of the two cytochrome oxidases *in vivo* can be gained.

*Table 2 – Energetic Profile of C. glutamicum: The listed theoretical ATP yields are based on the complete oxidation of one mol glucose, i.e. they are calculated for non-growing cells. In contrast to that, the maximal and effective in vivo ATP yields are determined based on the fluxome gained by ^{13}C-MFA for growing cells. The maximal in vivo ATP yield represents the in vivo potential reached when all reducing equivalents (NADH and MQH_2) supplied by the central carbon metabolism are converted to ATP, while the effective in vivo ATP yield (of the wild type) is based on the proton needs of the ATP synthase, as calculated based on the fluxome in combination with $Y_{ATP/Biomass}$. Hence, the maximal in vivo ATP yield limits the range for the effective in vivo ATP yield, i.e. the supplied reducing equivalents enable a higher proton translocation than required for growth. Columns marked with * are based on the assumption that the ATP synthase requires 4 H^+ for the formation of one ATP. Moreover, for the maximal in vivo ATP yield it is taken into account that the succinate dehydrogenase is a proton driven reaction and, thus, this reaction reduces the pmf by 2H^+ per one molecule fumarate formed [4]. The listed maintenance values are taken from [21].*

***C. glutamicum* ATCC 13032**								
Maintenance	GAM: 7.74 ± 0.16 mmol $_{Glucose}$ g_{CDW}^{-1}/ NGAM: 0.08 ± 0.02 mmol $_{Glucose}$ g_{CDW}^{-1} h^{-1}							
ATP/g_{CDW}	58.925 ± 5 mmol $_{ATP}$ g_{CDW}^{-1}							
		ATP by SLP	*NADH+ MQH_2*	*H^+*	*ATP by ETP**	*SLP:ETP ratio*	*total ATP*	*P/O ratio**
Maximal theoretical ATP yield	*bd* branch	4	10^T	16	4	50:50	8	0.5
	bc_1-aa_3 branch			56	14	22:78	18	1.5
Maximal *in vivo* ATP yield	*bd* branch	2.7	4.7^W	8.1	2.0	57:43	4.7	0.5
	bc_1-aa_3 branch			26.8	6.7	29:71	9.4	1.5
Effective *in vivo* ATP yield		2.7	1.7	8.8	2.2	55:45	4.9	0.5
Deviation (%) between effective and maximal *in vivo* yield		100%		32,7%	32,7%		52,1%	
***C. glutamicum* ΔF_1F_O**								
Maintenance	GAM:12.86 ± 0.46 mmol $_{Glucose}$ g_{CDW}^{-1}/ NGAM:0.19 ± 0.04 mmol $_{Glucose}$ g_{CDW}^{-1} h^{-1}							
ATP/g_{CDW}	58.925 ± 5 mmol $_{ATP}$ g_{CDW}^{-1}							
		ATP by SLP	*NADH+ MQH_2*	*H^+*	*ATP by ETP**	*SLP:ETP ratio*	*total ATP*	*P/O ratio**

Maximal theoretical ATP yield	*bd* branch	4	10^T	16	0	100:0	4	-
	bc_1-aa_3 branch			56	0	100:0	4	-
Maximal *in vivo* ATP yield	*bd* branch	3.4	6.2^M	10.3	0	100:0	3.4	-
	bc_1-aa_3 branch			35.1	0	100:0	3.4	-
Effective *in vivo* ATP yield		3.4	0	-	0	100:0	3.4	-
^{T} 10=6 NADH+4 MQH_2 ^{W} 4.7=3.3 NADH+1.4 MQH_2 ^{M} 6.2=4.1 NADH+2.1 MQH_2								

2. Materials & Methods

2.1. Bacterial strains and culture conditions

The strains used in this study were *C. glutamicum* ATCC 13032 and *C. glutamicum* ΔF_1F_O [13]. For both *C. glutamicum* strains, glucose-limited chemostat cultivations were performed under identical conditions. The strains were precultivated (inoculation with colonies from defrosted cryo cultures) in shake flasks at 30°C and 150rpm in CGXII medium containing 20 g l^{-1} glucose. After 15h of cultivation 50ml of the cell suspension was transferred into a 300ml aerobic stirred tank bioreactor (DASGIP GmbH, Jülich, Germany) containing 200 ml CGXII medium with 5 gl^{-1} glucose as sole carbon source (dilution rate of 0.15 h^{-1}). Cells were grown at 30°C at a constant pH of 7 and a dissolved oxygen concentration of >30%. The process parameters were monitored and if necessary adjusted by the software DASGIP Control 4.0. When glucose was depleted, i.e. if the residual glucose concentration falls below 2 g l^{-1}, the chemostat cultivation was started by addition of fresh CGXII medium with 5 g l^{-1} glucose as the growth-limiting substrate. Both strains form no acetate or other by-products when grown under glucose-limited conditions (the absence of acetate was confirmed by HPLC measurement). For further details, see supplement.

2.2. Carbon labeling experiments and mass spectrometry

Carbon labeling experiments (CLE) for the two strains *C. glutamicum* ATCC 13032 and *C. glutamicum* ΔF_1F_O were performed in three biological replicates each. Two different tracer mixtures were used, which were selected to provide optimal flux precision (see Sec. Computational ^{13}C MFA). Per strain, two CLEs were performed with a mixture consisting of 67% fully labeled glucose and 33% ^{12}C glucose and one CLE with a mixture of 63% fully labeled U-^{13}C glucose and 37% 1-^{13}C glucose. After 3.5 residence times samples were taken in six technical replicates, and processed for the subsequent measurement by LC-ESI-MS/MS to extract the mass isotopomer distribution data set for both strains. Measured metabolites were evaluated according to the protocols given in [22, 23]. For further details, see supplement.

2.3. Computational ^{13}C-MFA: network model and flux estimation

One biochemical reaction network describing the central metabolic pathways of both *C. glutamicum* strains was set up comprising reactions from EMP, PPP, TCA cycle, anaplerotic reactions, routes for glucose uptake and amino acid production as well as the biomass composition [24]. Because the *C. glutamicum* wild type (*C. glutamicum* ATCC 13032) and the *C. glutamicum* ΔF_1F_O deletion mutant share the same reactions within the scope of the model, i.e., the central carbon metabolism, the same network structure was used for modeling both strains. The model contains 52 metabolites and 84 reactions (17 thereof reversible). For detailed information on model reactions, directionalities, carbon atom transition, biomass composition and constraints the reaction network is attached as supplement in FluxML language [25].

The remaining steps were independently performed for *C. glutamicum* ATCC 13032 and *C. glutamicum* ΔF_1F_O. For the estimation of intracellular reaction rates, mass isotopomer data of intracellular metabolites as well as extracellular rates were integrated into the model. Global iterative flux estimation was performed according to

the workflow described in [26]. Applying a multi-start-strategy (MSO) with 1,000 randomly sampled optimization runs ensures finding a global flux optimum. All computations were done with the high-performance simulation software 13CFLUX2 [27].

2.4. Constraint-based analysis using a genome-scale model of C. glutamicum

Flux Balance Analysis (FBA) was performed using the genome-scale model of *C. glutamicum* ATCC 13032 [20] consisting of 475 metabolic reactions and 408 metabolites. The flux space was constrained to the phenotypes representing growth on glucose with an appropriate CO_2 formation. Strain specific maintenance values [21] as well as further constraints on intracellular fluxes (as determined by ^{13}C MFA analysis) were added (further details are given in the supplement). For the network, net flux distributions were calculated by FBA using growth as cellular objective for the linear programming problem [28-30]. All FBA-related simulations were performed using the COBRA toolbox with the LP solver GLPK and MATLAB (R2014a; Mathworks) [31, 32].

3. Results

3.1. Chemostat cultivations and carbon labeling experiments

The goal of this flux analysis study is to determine the ATP requirement for biomass formation ($Y_{ATP/Biomass}$) as a cornerstone for developing the full energetic profile of *C. glutamicum* growing under aerobic conditions. Particularly, the energetic efficiency of *C. glutamicum* can be analyzed by unraveling the proportions of ATP synthesis from SLP and ETP when comparing the wild type with the *C. glutamicum* ΔF_1F_O mutant. In the experimental setup, chemostat cultivations of *C. glutamicum* ATCC 13032 and *C. glutamicum* ΔF_1F_O were performed. Both strains were grown in CGXII minimal medium

under glucose-limited conditions. The dilution rate was set to D=0.15 h^{-1} using approximately 5 g L^{-1} glucose.

The cultivation data show phenotypic differences between both strains. The average value of the measured glucose uptake rates (GUR) of *C. glutamicum* ΔF_1F_O is increased by a factor of 1.74 (3.16 ± 0.33 mmol g_{CDW}^{-1} h^{-1} vs. 1.82 ± 0.15 mmol g_{CDW}^{-1} h^{-1}). This means that *C. glutamicum* ΔF_1F_O has to take up more glucose to reach the given wild type growth rate, i.e. *C. glutamicum* ΔF_1F_O has a smaller $Y_{X/S}$ than the WT. This difference between the glucose uptake rates of *C. glutamicum* ΔF_1F_O and the *C. glutamicum* wild type under glucose-limited conditions is smaller than previously reported, when the strains were grown under glucose excess conditions. Under glucose excess conditions the GUR of the ΔF_1F_O mutant was increased by up to 3.7 in the initial growth phase [13].

3.2. In vivo flux maps of C. glutamicum WT and C. glutamicum ΔF₁F₀

Figure 2 shows the net flux distribution for the *C. glutamicum* wild type as determined by ^{13}C metabolic flux analysis (flux values are expressed in absolute and relative numbers, i.e. as molar percentages of the specific uptake of glucose). Notice that flux estimation by ^{13}C MFA considers all raw data to have a measurement error. Thus, the measured extracellular fluxes are reconciled to obtain a stoichiometrically consistent result. For this reason, the rate estimates by ^{13}C MFA differ slightly from the measured ones.

In the following, the ^{13}C MFA estimated fluxes are used as the basis for discussion. It should be kept in mind that this is the global optimum of the underlying multi-start strategy. Moreover, it is common to lump reaction steps. This also effects the SLP reactions (glyceraldehyde-3-phosphate dehydrogenase and phosphoglycerate kinase are designated together with *gapA;* oxoglutarate dehydrogenase and succinyl

Coenzyme A synthetase are designated together with *odh*). One important branch point related to SLP is that of PPP versus glycolysis. The wild type flux distribution shows a relative PPP flux (represented by the 6-phosphogluconate dehydrogenase - *gnd* - net flux) of 52 ± 3% mmol $(mmol_{GLC})^{-1}$, which agrees well with literature values [33]. Likewise, the flux through the TCA cycle (represented by its entry flux through citrate synthase *gltA*) of 75 ± 3% mmol $(mmol_{GLC})^{-1}$ agrees with the values found in [34]. In total 53% of the carbon uptake is used for biomass formation. Since two thirds of the carbon used for biomass formation is located upstream of the TCA and some CO_2 is lost in PPP the TCA flux is only 75% of glucose influx despite flux doubling in lower glycolysis.

The net flux distribution of *C. glutamicum* ΔF_1F_O is visualized in Figure 3 and exhibits a relative flux into the PPP of 34 ± 3% mmol $(mmol_{GLC})^{-1}$. This *gnd* flux is smaller than that predominantly found in literature, ranging from 45% (pyruvate kinase deficient lysine producer) [35] to 113% (valine producer) [36]. In contrast, the flux through the TCA cycle (given by *gltA*) is with 114 ± 3% mmol $(mmol_{GLC})^{-1}$ higher than reported literature values, which are in the range of 42% - 83% mmol $(mmol_{GLC})^{-1}$ [37, 38]. However, for *C. glutamicum* grown at lower growth rates comparable values were found before [unpublished observation (Miebach 2011)].

The ^{13}C MFA estimated glucose uptake rate (*glc_upt*) of the ΔF_1F_O mutant (2.85±0.06 mmol g_{CDW}^{-1} h^{-1}) is 1.6 times higher than that found for the wild type (1.78±0.04 mmol g_{CDW}^{-1} h^{-1}). At the same time, the mutant uses less carbon for biomass formation, namely 37% in *C. glutamicum* ΔF_1F_O as compared to 53% for *the* wild type. This shift in carbon usage reflects the need of the mutant strain to produce ATP solely by SLP and, thus, less carbon is available for biomass formation.

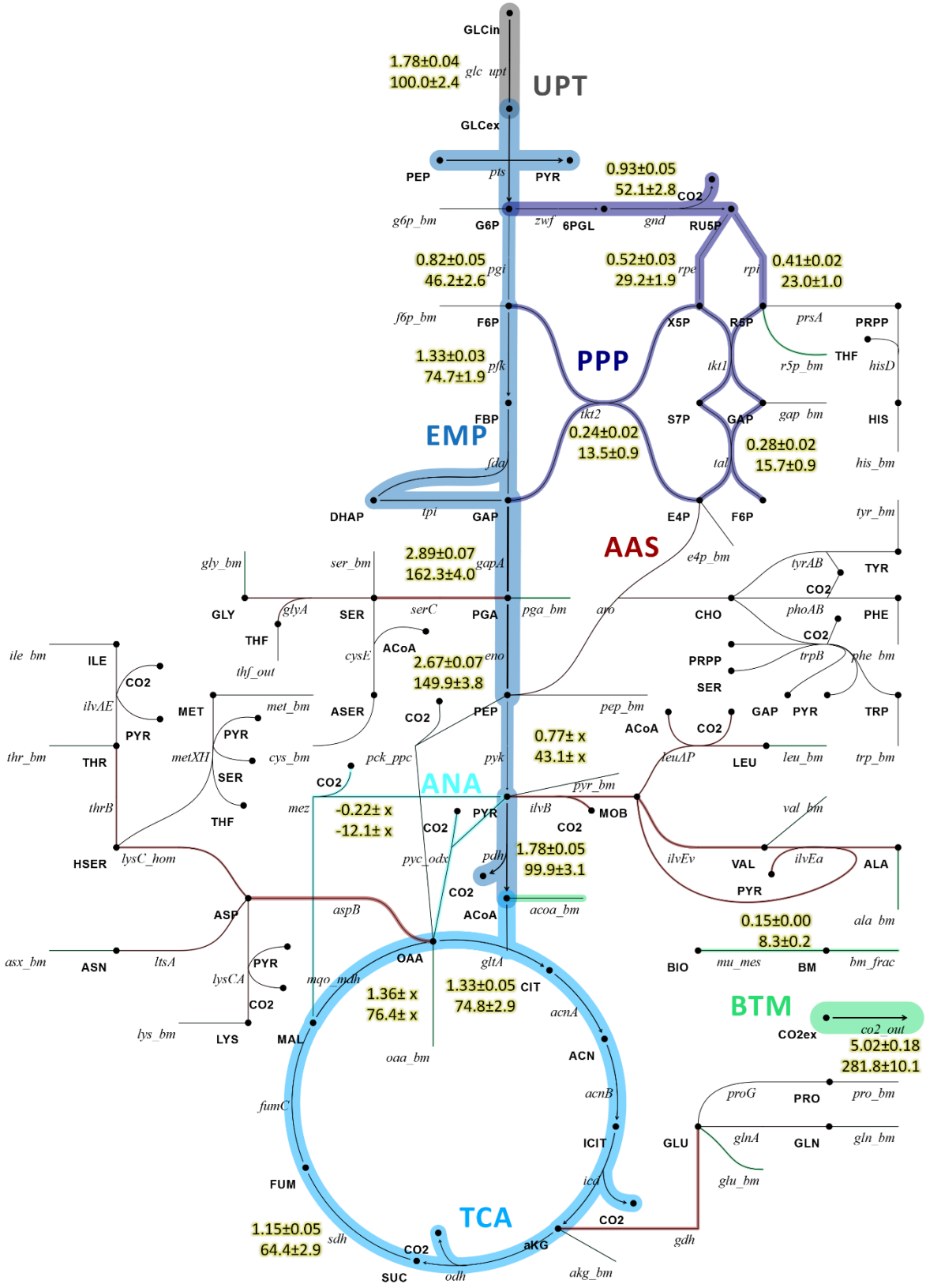

Figure 2: Flux map of C. glutamicum WT: Estimated intracellular flux distribution of C. glutamicum wild type applying isotopic stationary ^{13}C metabolic flux analysis. Flux values for selected reactions are given in absolute (mmol g_{CDW}^{-1} h^{-1}) and relative numbers, i.e relative means given as molar percentage of the glucose uptake. The

supplement gives the full reaction list with flux values including errors as well as enzyme long names.

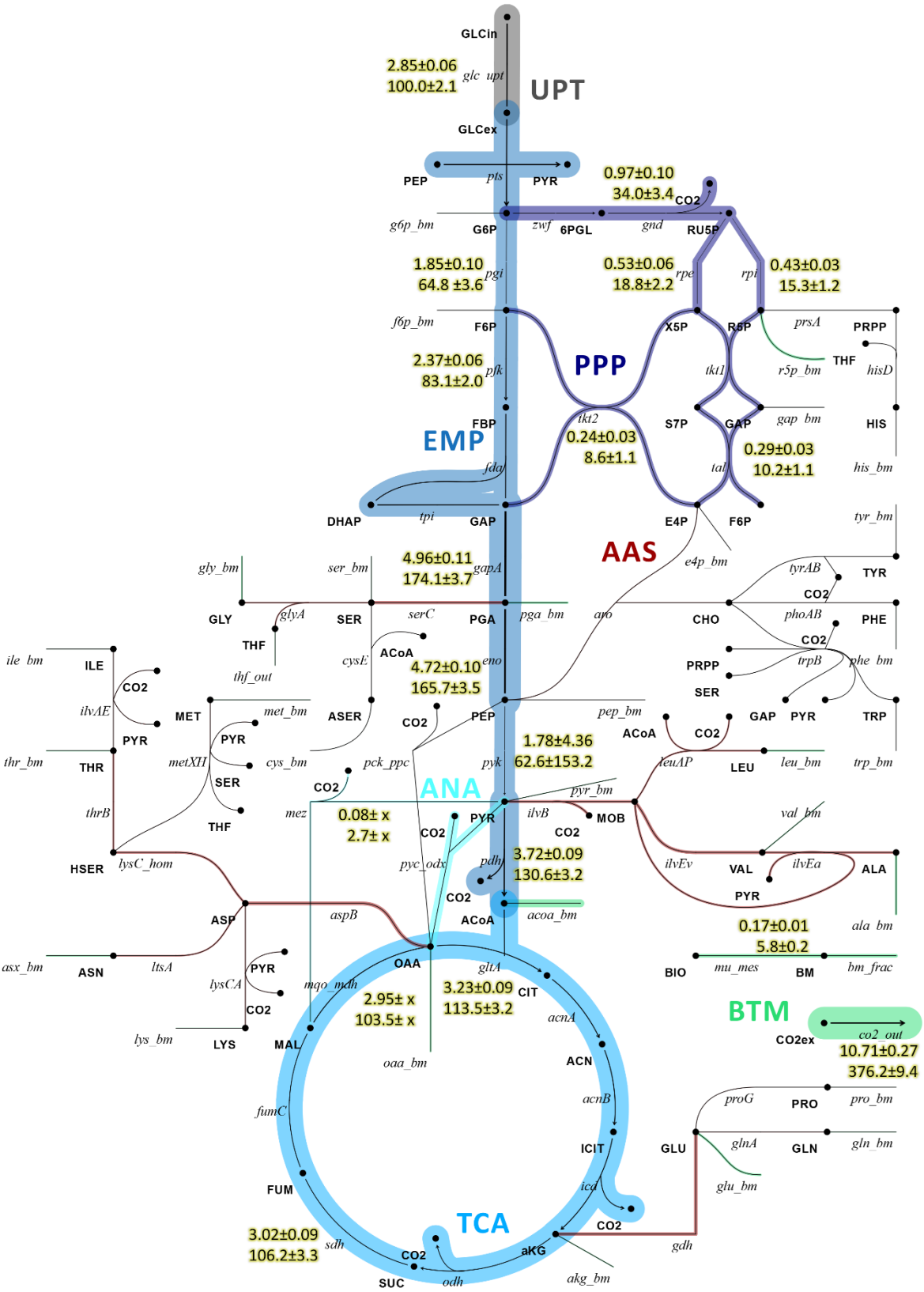

Figure 3: Flux map of C. glutamicum ΔF₁F₀: Estimated intracellular flux distribution of C. glutamicum ΔF₁F₀ applying isotopic stationary ^{13}C metabolic flux analysis. Flux

values for selected reactions are given in absolute (mmol g_{CDW}^{-1} h^{-1}) and relative numbers, i.e relative means given as molar percentage of the glucose uptake. The supplement gives the full reaction list with flux values including errors as well as enzyme long names.

3.3. Characteristic bioenergetic parameters

The flux distributions of the *C. glutamicum* wild type and ΔF_1F_O are now used to calculate the amount of ATP needed for biomass formation ($Y_{ATP/Biomass}$), the proportion of SLP and ETP in ATP formation, and the usage of pmf. By compiling these numbers, the full energetic profile of *C. glutamicum* is obtained (*Table 2*).

As confirmed by HPLC measurement (see supplement) both strains form no acetate or other by-products, thus, not showing overflow metabolism under glucose-limited conditions. In particular, the flux over acetate kinase (*ackA*) does not contribute to ATP synthesis by SLP. Accordingly, three SLP reactions remain for ATP synthesis: phosphoglycerate kinase and pyruvate kinase (glycolysis) and succinyl-CoA synthetase (TCA cycle).

Because *C. glutamicum* ΔF_1F_O can generate ATP exclusively by SLP, fluxes for all ATP producing reactions are available from ^{13}C MFA (see supplement). Our analysis shows that 51% of the produced ATP is formed by the phosphoglycerate kinase, succinyl-CoA synthetase makes up 31% and the remaining 18% are formed by the pyruvate kinase (Figure 4). Although, the statistical reliability of the pyruvate kinase reaction is unsatisfactory the trustworthiness of the $Y_{ATP/Biomass}$ value is reinforced by the MSO findings. With the metabolic fluxes of the ATP-producing SLP reactions at hand, it is now possible to calculate $Y_{ATP/Biomass}$ to be 59 ± 5 $mmol_{ATP}/g_{CDW}$, accounting for biomass formation as well as maintenance. Expressed in another way this

corresponds to 30 g ATP required for synthesis of 1 g of cells. Here as well the variability of the MSO results is alike (ranging from 50 to 63 $mmol_{ATP}/g_{CDW}$), showing that the organism-specific value as determined by MFA is lower than the rough estimation (of 100 $mmol_{ATP}/g_{CDW}$) previously assumed.

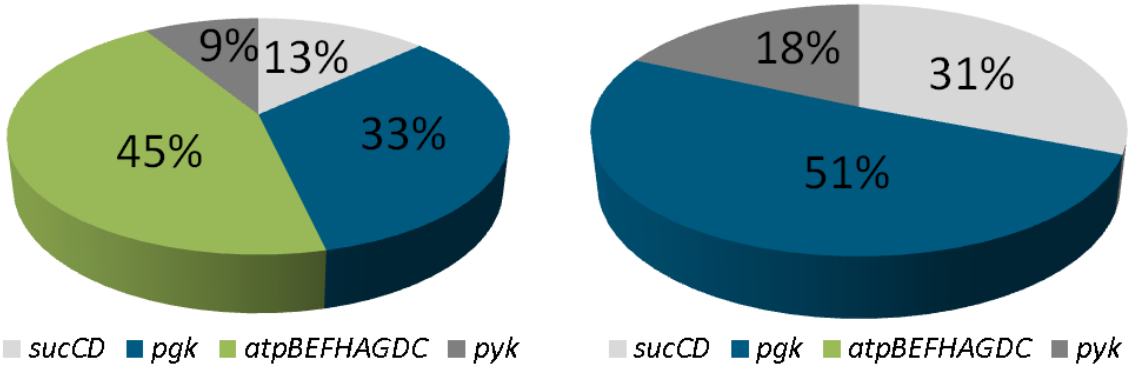

Figure 4: Impact of ETP and SLP on ATP production: Composition of ATP-producing reactions as given by the flux distribution determined for C. glutamicum wild type (left) and C. glutamicum ΔF₁F₀ (right) grown under glucose-limited conditions.

In analogy to the calculation of $Y_{ATP/Biomass}$ the efficiency of substrate usage can be determined by relating the total amount of generated ATP to the GUR. As *C. glutamicum* ΔF_1F_O can solely produce ATP by SLP, the maximal theoretical ATP yield per glucose molecule is five at most (cf. Introduction). In contrast to this maximal value (which is achieved by oxidizing glucose without any biomass formation), the *in vivo* flux distribution reveals that *C. glutamicum* ΔF_1F_O generates an effective *in vivo* yield (not taking into account the ATP consumed by phosphofructokinase) of 3.43 ± 0.14 ATP per glucose. Referred to the maximal theoretical yield of 5 ATP this corresponds to an *in vivo* loss of about 31% of ATP which is primarily explained by carbon loss in the PPP pathway as well as some biomass effluxes in glycolysis.

Because both strains are viable and all biomass precursor metabolites from central metabolism are available, it is reasonable to assume that both strains require the same amount of ATP for biomass synthesis. There is no obvious reason that would suggest

that the biomass composition of the mutant is different from the wild type. Accepting this assumption, the $Y_{ATP/Biomass}$ value calculated for the ΔF_1F_O mutant can be adopted for the wild-type strain and bioenergetics calculations can be performed for the *C. glutamicum* wild type. First, the $Y_{ATP/Biomass}$ value enables the calculation of the ATP synthase flux (*ATPase*) from the following balance:

$$ATPase = Y_{ATP/Biomass} * \mu - (gapA + pyk + odh)$$

Remember that the identifiers designate lumped reactions (*gapA*: phosphoglycerate kinase, *odh*: succinyl Coenzyme A synthetase). Based on the calculated $Y_{ATP/Biomass}$ the minimal flux over ATP synthase (required to achieve $Y_{ATP/Biomass}$) is 3.9 ± 0.7 mmol $g_{CDW}^{-1}h^{-1}$. Related to the glucose uptake, this corresponds to 2.2 ATP produced by ETP per glucose molecule (Table 2). Collating this ATP synthase flux to the supplied reducing equivalents achieves a corresponding proton translocation of 2.15 $H^+/2e^-$. Furthermore, relating this ATP synthase flux to the fluxes of the SLP reactions (*gapA*, *pyk*, *odh*) as determined by ^{13}C MFA for the *C. glutamicum* wild type, reveals that roughly half (45%) of the ATP is produced by ATP synthase followed by phosphoglycerate kinase with 33%, whereas succinyl-CoA synthetase and pyruvate kinase each make up approximately 10% (Figure 4). Again the reliability of the values is reinforced by performing MSO. This SLP-ETP ratio (of 55:45) implies that ETP and SLP equally contribute to ATP synthesis.

The *in vivo* flux map and the calculated ATP synthase flux of the wild type also enable the estimation of the efficiency of substrate usage (i.e. moles ATP per mol glucose). It turns out that *C. glutamicum* wild type generates 4.9 ± 0.78 ATP per glucose, which is much lower than the maximal theoretical ATP yield of *C. glutamicum* of 18 ATP per glucose molecule (cf. Introduction). Thereof, the SLP contributes 2.7 ATP per glucose

molecule, which is 54% less than the 5 ATP that could be maximally generated by SLP.

3.4. In silico characterization of the energy metabolism by a genome-scale model

The results obtained by ^{13}C MFA are now put into the global context of a genome-wide network model in order to study the energetic efficiency of *C. glutamicum*. In consequence, the combination respectively comparison of ^{13}C MFA and FBA reveals limiting reactions. Moreover, FBA allows identifying at least a window of realistic proportions in which the two terminal oxidases probably operate.

In accordance with the ^{13}C MFA flux map growth on glucose (with appropriate CO_2 formation) was achieved by setting adequate constraints. To this end, all calculated fluxes of the central carbon metabolism were restricted as given by the ^{13}C MFA flux map. Thereby the standard deviations of the flux rates are taken into account by specifying upper and lower bounds for each flux. Likewise, the maintenance requirements were restricted to strain specific values given by [21].

Clearly, if only the extracellular fluxes are taken into account the genome wide model permits many possible flux distributions which are stoichiometrically consistent and reproduce the measured external fluxes (GUR, CO_2 excretion rate, and growth rate). FBA just selects one of these distributions by maximizing some given criterion, in this study the growth rate. Thus, FBA – in a positive sense – can only produce an educated guess of the real *in vivo* flux distribution based on measured extracellular flux data.

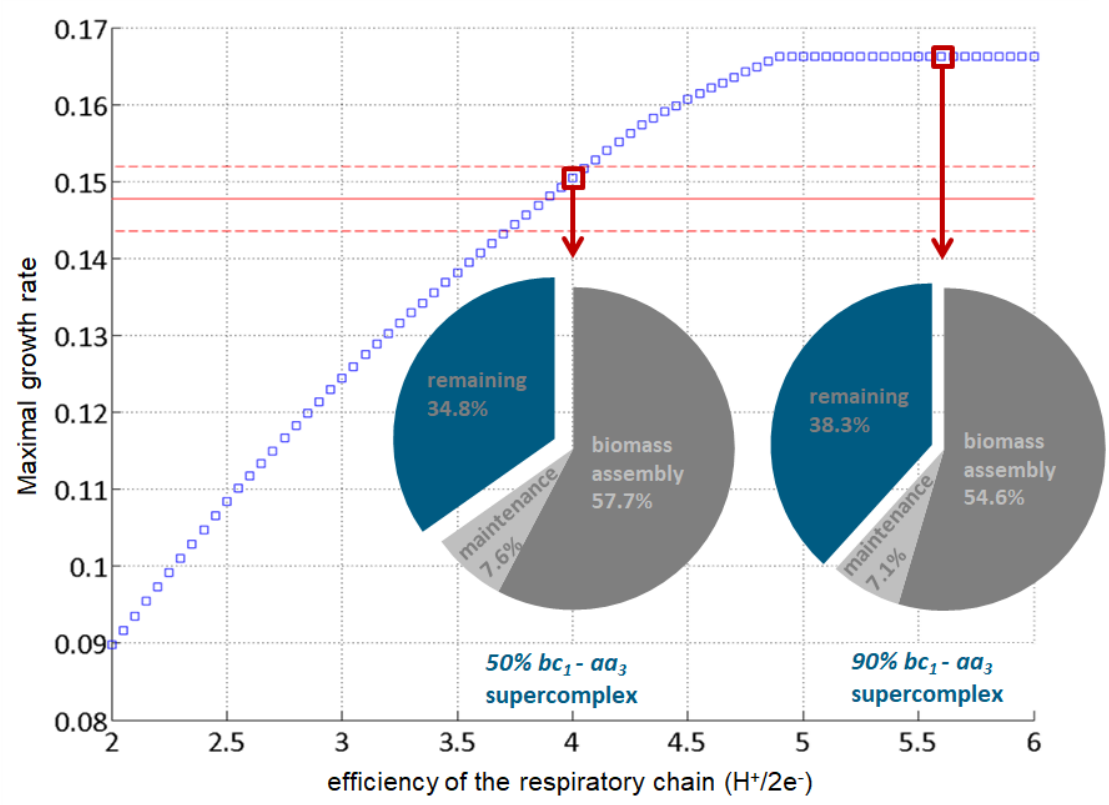

Figure 5: Growth rate as predicted by flux balance analysis (FBA) with maximizing growth rate as objective using the genome wide network model of C. glutamicum. Fluxes of the central carbon metabolism were restricted as given by the ^{13}C MFA fluxome taking into account the standard deviations of the flux rates. Furthermore, the maintenance requirements were restricted to strain-specific values given by [21]. The stoichiometric coefficient ($H^+/2e^-$) of the oxidase reactions (which can lie between 2 and 6) was shifted between the two extremes 6 (solely bc_1-aa_3 supercomplex) and 2 (solely bd oxidase) representing a reduction of the bc_1-aa_3 supercomplex activity and simultaneously an increase of the bd oxidase activity. For oxidase ratios of 50% ($4H^+$/ATP) and 90% ($5.6H^+$/ATP) the ATP-consuming reactions of the FBA predicted flux maps were analyzed in more detail, i.e. it was quantified which portion is used for biomass assembly (from supplied precursors), maintenance and futile cycling.

Inserting also the intracellular flux values calculated by ^{13}C MFA in the genome wide network tremendously reduces the space of possible flux distributions consistent with the data. But, there still remain several degrees of freedom. One reason is that the electron transport chain is not part of the underlying smaller carbon flux model and, thus, the usage of the two oxidases is only in the scope of the larger model.

Moreover, putting the ^{13}C MFA-derived flux map in the context of the genome wide stoichiometry allows for linking the supply of energetic cofactors to cell maintenance. In particular, the usage of the strain-specific maintenance values, for both, growth (GAM) and non-growth associated maintenance (NGAM), is a crucial step when aiming at a comprehensive description of the energy metabolism. Here, overestimating the maintenance requirements implies too high ATP needs and, thus, prevents an accurate evaluation of the energy metabolism. It should be remarked that the model by Kjeldsen et al. [34], which provided the basis for our model, relies on relatively high values for growth associated maintenance (19 mmol g_{CDW}^{-1}). The values reported in [21] for *C. glutamicum* wild type were, however, 65% lower than those given by Kjeldsen et al. Therefore, the maintenance values of the genome-wide network model were adjusted to the experimentally determined strain-specific values reported for *C. glutamicum* [21].

The genome wide network model of *C. glutamicum* with updated maintenance values and constrained by ^{13}C MFA fluxes was used to examine the findings concerning the contribution of the ETP for overall ATP synthesis as well as the portion of pmf used for ATP synthesis. This was done by employing FBA.

When restricting the reactions according to the ^{13}C MFA results (including the growth rate) the observed growth rate of 0.15 h^{-1} can be emulated.

In a next step, we investigated which range of ratios of the two terminal oxidases allow for a growth rate of 0.15 h^{-1}. The stoichiometric coefficient ($H^+/2e^-$) of the oxidase reaction can take a value between two and six, representing sole use of the *bd* oxidase and the bc_1-aa_3 supercomplex, respectively. Therefore, the coefficient was varied between the two extremes six and two corresponding to an increase of the *bd* oxidase and simultaneously a reduction of the bc_1-aa_3 supercomplex. We find that the usage

of the bc_1-aa_3 supercomplex in a range of 43%-100% still allows for a growth rate of 0.15 h^{-1} as given by the ^{13}C MFA flux map (Figure 5). This oxidase ratio of 43% bc_1-aa_3 supercomplex and 57% *bd* oxidase complies with a proton translocation of 3.7 $H^+/2e^-$. When further increasing the supercomplex ratio, the growth rate even increased further (beyond the set flow rate). However, due to the settings of intracellular fluxes, the maximal FBA predicted growth rate is 0.168 h^{-1}. In contrast, when reducing the $H^+/2e^-$ ratio to the value of 2.15 required for achieving the minimal flux over the ATP synthase in *C. glutamicum* as forecasted by the ^{13}C MFA flux map, the growth rate reaches only ~65% of the growth rate adjusted in the labeling experiments. This is not a contradiction because the minimal proton requirements of ATP synthase (2.15 $H^+/2e^-$) probably underestimate the actual proton translocation. Moreover, the fact that a *C. glutamicum Δqcr* mutant is able to grow, although at a 45% decreased growth rate [20], shows that the *bd* oxidase alone is sufficient to generate enough ATP. So far, the analysis has been limited mainly to ATP production. Furthermore, Figure 5 highlights the use of ATP in the genome-wide model. Due to the non-unique reaction assignment to anabolism or catabolism the grouping must be arbitrary. Therefore, the biomass assembly reactions from supplied precursors were grouped, while all reactions upstream to biomass precursors where assigned to ‘rest’. The biomass assembly uses ~ 58%, the maintenance requires ~7%, and the rest the remaining 35%. Thereof, the main consumer is the phosphofructokinase using approximately 9% of the total ATP produced. Thus, FBA generates a more detailed understanding of the ATP usage because it enables to separate the NGAM requirements from the global energy budget.

4. Discussion

4.1. Effective ATP requirements of biomass formation

Previous studies on ATP yields for non-fermentative organisms heavily relied on theoretical considerations. The major aim of the work presented here was to elucidate the energy metabolism of *C. glutamicum* experimentally by comparing flux distributions of *C. glutamicum* wild type (using SLP and ETP) and *C. glutamicum* ΔF_1F_O (SLP only). Using state-of-the-art ^{13}C MFA, the comparison of the fluxome of both strains gave new insights into the energetic profile of *C. glutamicum*. The main advantage of ^{13}C MFA is that it generates key *in vivo* bioenergetic quantifiers without relying on additional assumptions with respect to energy metabolism [19]. In particular, it allows for a direct quantification of the SLP reactions and the reactions that supply the reducing equivalents NADH and MKH2. The most important result derived is the determination of the ATP requirement for biomass production ($Y_{ATP/Biomass}$) of *C. glutamicum*, which results from the specific biomass composition of the respective organism and, subsequently enables the characterization of further bioenergetics properties (at least for the glucose-limited case with $D=0.15h^{-1}$ discussed here). The effective *in vivo* ATP yield could be determined with the mutant strain *C. glutamicum* ΔF_1F_O that lacks the ATP synthase and thus can generate ATP only via SLP. Consequently, all ATP-producing reactions could by measured by ^{13}C MFA.

Previously, based on theoretical considerations, guesses for $Y_{ATP/Biomass}$ in *C. glutamicum* were in the order of 100 $mmol_{ATP}/g_{CDW}$. For other organisms, similar values were reported. This is the first study that reports an experimentally derived value for *C. glutamicum* by an integrative model-based approach, which combines ^{13}C MFA results with FBA using a large-scale stoichiometric network. Calculating $Y_{ATP/Biomass}$ for *C. glutamicum* reveals that 59 ± 5 mmol ATP are needed to synthesize one gram of

cell dry weight including maintenance requirements besides biomass formation. This experimentally determined $Y_{ATP/Biomass}$ value of *C. glutamicum* gives the first reliable value for judging the ATP efficiency of the organism. It is slightly smaller than values given in literature [16-18, 39] for other organisms.

With an anaplerotic node comprising six reactions (more than any other standard organism), it turned out, that for principal mathematical reasons the pyruvate kinase flux is in general not well resolvable in *C. glutamicum* by steady state ^{13}C MFA [40]. Although the pyruvate kinase flux is not determined with highest precision, there are good arguments why the $Y_{ATP/Biomass}$ value is reliable. The discussed flux map is the global optimum found by applying a multi-start strategy. Inspecting the spread of the flux values for all resulting (probably only local) optimal flux estimates of all optimization runs strengthens the trustworthiness. Furthermore, the $Y_{ATP/biomass}$ value for this flux range is alike.

Moreover, the $Y_{ATP/biomass}$ value is alike even if the relative PPP flux (and thus the ratio of PPP versus glycolysis) varies significantly between 9% and 34% mmol $(mmol_{GLC})^{-1}$. This shows the generality of the value for *C. glutamicum*, i.e. the strain-specific value is well restricted. Not knowing the $Y_{ATP/biomass}$ value from the mutant strain, would enable values from 57 to 113 $mmol_{ATP}/g_{CDW}$ spanned by the oxidases, which underlines the importance of the conducted experiments.

Previous studies reported, that ATP futile cycling plays a significant role in several platform organisms [41-44]. Because it is not possible to quantify the totality of all futile cycles in a living cell, the amount of wasted ATP is effectively contained in the calculated $Y_{ATP/Biomass}$ value. In this sense, $Y_{ATP/Biomass}$ might even overestimate the effective yield.

4.2. Effective in vivo impact of ETP and pmf

Although it is commonly assumed that ETP is predominantly responsible for aerobic ATP synthesis in *C. glutamicum*, Koch-Koerfges et al. [13] conjectured that the ATP synthesis by OxPhos is probably overvalued. This could be confirmed by our study, which revealed that the impact of OxPhos is actually overestimated. At the theoretical maximum, up to 78% of the ATP is synthesized by ETP. This is only a low fraction compared to mitochondria or other organisms (*Under physiological* conditions, it is not possible to say, which part of glucose is converted to energy, biomass or other products. The reason is that many reaction steps cannot be uniquely assigned to anabolism or catabolism. Consider, for example, the biomass precursor pyruvate, which generates only the ATP of SLP and the two NADH formed in glycolysis but not the reduction equivalents gained in the TCA cycle nor the ATP formed by succinyl-CoA synthetase. Only in the (theoretical) case of complete usage of glucose for ATP production, this problem does not arise. Under realistic conditions, however organisms have to balance the trade-off between biomass and energy formation. In this situation, effective yield coefficients relating glucose uptake to overall ATP and biomass production are the best way to characterize the catabolic versus anabolic branch.

Table 1). Flux analysis revealed that in the *C. glutamicum* wild type only 45% of the ATP is produced by ATP synthase.

This challenges the common opinion that under aerobic conditions ETP is the main source of ATP production. Furthermore, it confirms that the *bd* oxidase could be sufficient to serve the organism with an adequate amount of ATP for growth, however the maximal achievable growth rate is reduced [21]. Hence, the low effective *in vivo* ATP yield by ETP indicates that a significant fraction of pmf is needed for cellular processes like pH-homeostasis, maintenance, transport processes or lost by proton

leakage. Thus, *C. glutamicum* presumably utilizes pmf depending on the nutritional and environmental conditions where it must balance growth and other pmf-dependent processes.

For this reason, the pmf in *C. glutamicum* deserves a more detailed discussion. Electrons passed through the respiratory chain generate the pmf. Due to the branched nature of the respiratory chain, the exact amount of protons per electron transferred from the inside to the outside of the cell is unknown. Thus, the pmf can vary depending on the ratio in which the two terminal oxidases are used [21]. Starting point of pmf generation are the reducing equivalents (NADH and reduced menaquinone – MKH2), generated by the central carbon metabolism. Like the metabolic rates of SLP reactions, ^{13}C MFA determines the flux through the reactions that supply NADH and MKH2 (Figure 2). Because the NADH dehydrogenase (NDH) of *C. glutamicum* does not translocate protons [5, 45, 46], the oxidation of NADH and MKH2 results in the same H^+/e^- ratio. Nevertheless, it has to be taken into account that succinate dehydrogenase is a proton driven reaction and, thus, this reaction reduces the pmf by $2H^+$ per one molecule fumarate formed [4]. The amount of reducing equivalents supplied by the central carbon metabolism, as given by the *C. glutamicum* wild type flux distribution during growth on glucose, is 3.3 NADH and 1.4 MKH2 per glucose. These amounts of NADH and MKH2 enable translocation in the range from 8.1 to 26.8 protons depending on the ratio of *bd* oxidase and bc_1-aa_3 supercomplex and taking into account the proton influx required by the succinate dehydrogenase. This compares with the minimal ATP synthase flux (of 2.2 ATP per glucose molecule – `Table 2`) which requires 8.8 translocated protons (assuming that 4 H^+ are required for the synthesis of one ATP). For comparison, the ΔF_1F_O mutant flux distribution infers production of 4.1 NADH and 2.1 MKH2 per glucose, which could result in 10.3 protons (assuming that solely *bd* oxidase is used) to 35.1 protons (assuming that solely the bc_1-aa_3 supercomplex is

used). This confirms the finding reported in [13] that the ΔF_1F_O mutant shows increased pmf compared to the wild type.

This underpins that *bd* oxidase alone would almost be sufficient to supply the organism with ATP. A previous study, however, showed that the *bc*$_1$-*aa*$_3$ supercomplex is of major importance for aerobic respiration [13]. The difference between the supplied and required protons (26.8 vs. 8.8) confirms that the pmf is used for other cellular processes. To give an example: assuming that (i) 90% or (ii) 50% of the reducing equivalents are passed over the *bc*$_1$-*aa*$_3$ supercomplex (remaining portion passed over the *bd* oxidase) results in (i) 35% or (ii) 51% of the generated pmf used for ATP synthesis, while the remaining portion of the pmf is used for other cellular processes, e.g. pH homeostasis and transport processes. Besides direct proton deduction, it is also theoretically possible to convert the pmf totally to ATP and subsequently futile cycling wastes the ATP. Consequently, both the proton and the ATP loss will affect the magnitude of ATP dissipation via energy-spilling reactions [47].

Finally, it is important to mention that the observed phenomena were figured out under the special conditions of glucose limitation, oxygen excess and a growth rate of only 0.15 h^{-1}. The organism might face energetically more demanding conditions in its natural habitat, which require more ATP and hence a higher impact of the *bc*$_1$-*aa*$_3$ supercomplex.

4.3. Efficiency of substrate usage

Compared to the theoretical maximal ATP yield, the actual *in vivo* yield of both strains is lower. It turns out that the efficiency of substrate usage (yield in mol ATP/mol glucose) of *C. glutamicum* ΔF_1F_O is 3.4 ± 0.14 ATP/glucose, whereas the wild type generates 4.9 ± 0.78 ATP/glucose. Thereof, the SLP portion is 2.7 ATP/glucose, which corresponds to an effective *in vivo* ATP yield that is 51% lower than the theoretical

maximal ATP yield. In comparison with the mutant strain, where the ATP loss of the SLP is only 35%, which emphasizes the need of *C. glutamicum* ΔF_1F_O to use the scarce ATP supply more efficiently, while the wild type is more flexible due to the increased availability of ATP.

Furthermore, the ATP loss of the ETP is higher. Even when exploiting the full *in vivo* potential (reached when converting all reducing equivalents to ATP by using the bc_1-aa_3 supercomplex), the resulting effective *in vivo* ATP yield of the ETP is 6.7 ATP/glucose. Hence, the *in vivo* potential is ~50% smaller than the theoretical maximal ATP yield. The effective *in vivo* yield of the ETP (2.2 ATP/glucose), based on ATP synthase activity needed to reproduce the strain-specific $Y_{ATP/Biomass}$ value, is even lower as it uses only 33% of the *in vivo* potential. Accordingly, the effective P/O ratio is 0.54, which is as efficient as exclusively using the less efficient *bd* branch. Taking ETP and SLP together, the efficiency of substrate usage of the *C. glutamicum* wild type (4.9 ATP/glucose) is only 27.2% of the theoretical maximal ATP yield. Thereby, the carbon loss through the PPP is only ~10%. Hence, the main reason leading to a reduction of ATP formation is the anabolism, i.e. the carbon used for biomass formation. The wild type uses 53% of the glucose taken up for biomass formation. It is important to note that this carbon is not completely available for ATP formation. Depending on the accurate positioning of the biomass efflux, carbon can be used partially for ATP formation as well as for biomass formation.

4.4. The global metabolic context

The energetic properties were put into the global metabolic context by performing flux balance analysis with a genome-scale model of *C. glutamicum*. When narrowing down the flux rates to the values of the fluxes determined by ^{13}C MFA, a growth rate of 0.15 h^{-1} was emulated by FBA. Interestingly, in the genome wide model this growth rate of

0.15 h^{-1} could be achieved with different ratios of the two terminal oxidases as long as the *bc*$_1$-*aa*$_3$ supercomplex is used by up to 43%. This oxidase ratio complies with a proton translocation of 3.7 $H^+/2e^-$. This means that 14% of the ATP produced by ETP (9% of total ATP generated) is used for non-growth associated investments of the cell, represented by NGAM, and is, thus, not available for growth.

Concluding, this showed that FBA allows a more detailed understanding of ATP usage of *C. glutamicum* and provided realistic portions in which the two terminal oxidases probably are used.

For metabolic engineering applications, the findings advise that there is a potential to improve the energy conservation by ETP by overproduction of F_1F_O-ATP synthase (if the enzyme would operate at its maximum). Furthermore, the understanding of OxPhos can assist by enhancing ATP regeneration for amino acid synthesis especially of energy demanding amino acids.

4.5. Robustness with respect to oxygen fluctuations

The obtained results shed some new light on the remarkable robustness of *C. glutamicum* to external fluctuations of the oxygen availability as shown before also in [48]. In large-scale industrial bioreactors, such fluctuations cannot be prevented because of the limiting energy input for stirring [49, 50]. For simulating these conditions at lab scale, a scale down bioreactor setup was realized [51]. Herein, an aerated aerobic stirred tank reactor (STR) was coupled to a non-aerated plug flow reactor (PFR) in closed loop. In this arrangement, *C. glutamicum* cells have to pass the non-aerated zone in frequent cycles with narrow residence time distribution. During the passage remaining oxygen is consumed leading to oxygen depletion. It could be shown that up to a residence time of 180 seconds in the non-aerated zone no growth or

production phenotype could be observed for fed-batch operation for L-lysine as well as cadaverine producing *C. glutamicum* strain.

The reduced necessity to gain ATP from ETP could be one reason for *C. glutamicum'*s remarkable robustness to bioreactor inhomogeneity in large scale industrial processes. Such reduced dependence on respiration could allow for flexible switching from respiration to fermentation and back with negligible impact in terms of total ATP regeneration. For comparison, other organisms, like *Escherichia coli* [52-57], *Saccharomyces cerevisiae* [58, 59] and *Bacillus subtilis* [60] partial oxygen limitation and substrate limitation even for shorter time span led to an increased side product formation, consequently resulting in losses of biomass and product formation.

This remarkable robustness, which specifically qualifies *C. glutamicum* for an industrial production host, is strongly supported and partially explained by the findings of the present investigation.

4.6. Method transferability

It should be pointed out that the general approach taken in this investigation should also work for other industrial platform organisms provided it is possible to knock out the ATP synthase while still maintaining a moderate aerobic growth. In addition to *C. glutamicum*, up to now, it could be shown for *E. coli* and *B. subtilis* that the F_1F_O-ATP synthase is not essential for growth [13, 61, 62] whereas for *Mycobacterium tuberculosis* and *M. smegmatis* the F_1F_O-ATP synthase is essential [63-66]. A comparison of the ΔF_1F_0 mutants of *E. coli*, *B. subtilis*, and *C. glutamicum* revealed many similarities, indicating that many of the conclusions drawn here for *C. glutamicum* are valid for the two other bacterial species, too [13].

Even for organisms in which the ATP synthase is essential ^{13}C -MFA can provide valuable information for understanding the process of respiration. Quantifying the SLP

reactions as well as those supplying reducing equivalents shed more light on the range of ATP generated in vivo, by showing how far the in vivo flux is below the theoretical considerations.

However, the observation that there is a diversity of electron transport chain composition, especially the existence of multiple terminal oxidases, shows that transferring the approach to other bacteria will face the same restrictions. A way out is given by the respiratory chain mutants described in [21]. As the strain *C. glutamicum* Δ*cydAB* and *C. glutamicum* Δ*qcr* can each use only one of the terminal oxidases, they have a defined H^+/e^- ratio. Hence, in this case, the analysis is simpler because the problem of terminal oxidases with different H^+/e^- ratios does not occur.

Conflict of interest

The authors declare that they have no conflict of interest.

Author Contributions

MB triggered the study. NP conducted the lab experiment. NP, EZ and KN analyzed data sets. EZ and KN designed the modelling. EZ performed the computational analyses. All authors discussed the results. KN, MO, and WW supervised and guided the project. EZ and WW wrote the manuscript to which KN, MO, and MB contributed. All authors approved the content of the manuscript.

Acknowledgements

The authors would like to thank Petra Geilenkirchen and Matthias Moch for excellent technical assistance. The German Federal Ministry of Education and Research (grant number 0315598A, BMBF, Berlin, Germany) partially funded this work.

References

1. Litsanov, B., M. Brocker, and M. Bott, *Toward homosuccinate fermentation: metabolic engineering of corynebacterium glutamicum for anaerobic production of succinate from glucose and formate.* Applied and Environmental Microbiology, 2012. **78**: p. 3325-3337.
2. Eggeling, L. and M. Bott, *A giant market and a powerful metabolism: L-Lysine provided by Corynebacterium glutamicum.* Applied microbiology and biotechnology, 2015. **99**(8): p. 3387 - 3394.
3. Becker, J. and C. Wittmann, *Advanced Biotechnology : Metabolically Engineered Cells for the Bio-Based Production of Chemicals and Fuels , Materials , and Health-Care Products.* Angewandte Chemie (International ed. in English), 2015. **54**: p. 3328-3350.
4. Bott, M. and A. Niebisch, *The respiratory chain of Corynebacterium glutamicum.* Journal of Biotechnology, 2003. **104**: p. 129-153.
5. Maeda, T., A. Koch-Koerfges, and M. Bott, *Relevance of NADH Dehydrogenase and Alternative Two-Enzyme Systems for Growth of Corynebacterium glutamicum With Glucose, Lactate, and Acetate.* Frontiers in Bioengineering and Biotechnology, 2021. **8**.
6. Kabus, A., A. Niebisch, and M. Bott, *Role of cytochrome bd oxidase from Corynebacterium glutamicum in growth and lysine production.* Applied and Environmental Microbiology, 2007. **73**: p. 861-868.
7. Niebisch, A. and M. Bott, *Purification of a cytochrome bc-aa3 supercomplex with quinol oxidase activity from Corynebacterium glutamicum. Identification of a fourth subunity of cytochrome aa3 oxidase and mutational analysis of diheme cytochrome c1.* The Journal of Biological Chemistry, 2003. **278**(6): p. 4339-4346.
8. Stock, D., A.G.W. Leslie, and J.E. Walker, *Molecular architecture of the rotary motor in ATP synthase.* Science, 1999. **286**: p. 1700-1705.
9. Watt, I.N., et al., *Bioenergetic cost of making an adenosine triphosphate molecule in animal mitochondria.* Proceedings of the National Academy of Science of the USA, 2010. **107**: p. 16823-16827.
10. Ferguson, S.J., *ATP synthase: from sequence to ring size to the P/O ratio.* Proceedings of the National Academy of Science of the USA, 2010. **107**: p. 16755-16756.
11. Hinkle, P.C., *P/O ratios of mitochondrial oxidative phosphorylation.* Biochimica et biophysica acta, 2005. **1706**: p. 1-11.
12. Munk, K., *Die Atmungskette*, in *Taschenlehrbuch Biologie: Biochemie - Zellbiologie*. 2008, Thieme: Stuttgart. p. 300-313.
13. Koch-Koerfges, A., et al., *Physiology and global gene expression of a Corynebacterium glutamicum ΔF(1)F(O)-ATP synthase mutant devoid of oxidative phosphorylation.* Biochimica et biophysica acta, 2012. **1817**: p. 370-80.
14. Käß, F., et al., *Process inhomogeneity leads to rapid side product turnover in cultivation of Corynebacterium glutamicum.* Microbial cell factories, 2014. **13**(1): p. 6 -.
15. Stouthamer, A.H., *A theoretical study on the amount of ATP required for synthesis of microbial cell material.* Antonie Van Leeuwenhoek, 1973. **39**: p. 545-565.
16. Varma, A. and B.O. Palsson, *Stoichiometric flux balance models quantitatively predict growth and metabolic by-product secretion in wild-type Escherichia coli W3110.* Applied and Environmental Microbiology, 1994. **60**: p. 3724-3731.
17. Downs, A.J. and C.W. Jones, *Energy Conservation in Bacillus megaterium.* Archives of Microbiology, 1975. **105**: p. 159-167.
18. Verduyn, C., et al., *Energetics of Saccharomyces cerevisiae in anaerobic glucose-limited chemostat cultures.* Journal of General Microbiology, 1990. **136**: p. 405-412.
19. Wiechert, W. and A.A. de Graaf, *In vivo stationary flux analysis by 13C labeling experiments.* Advances in Biochemical Engineering/Biotechnology, 1996. **54**: p. 109-154.
20. Zelle, E., K. Nöh, and W. Wiechert, *Growth and Production Capabilities of Corynebacterium glutamicum: Interrogating a Genome-scale Metabolic Network Model*, in *Corynebacterium glutamicum From Systems Biology to Biotechnological Applications*. 2015, Caister Academic Press: Norfolk, UK. p. 39-55.

21. Koch-Koerfges, A., et al., *Conversion of Corynebacterium glutamicum from an aerobic respiring to an aerobic fermenting bacterium by inactivation of the respiratory chain.* Biochimica et biophysica acta, 2013. **1827**: p. 699-708.
22. Luo, B., et al., *Simultaneous determination of multiple intracellular metabolites in glycolysis, pentose phosphate pathway and tricarboxylic acid cycle by liquid chromatography-mass spectrometry.* Journal of Chromatography, 2007. **1147**: p. 153-64.
23. Paczia, N., et al., *Extensive exometabolome analysis reveals extended overflow metabolism in various microorganisms.* Microbial Cell Factories, 2012. **11**: p. 122.
24. Marx, A., et al., *Determination of the fluxes in the central metabolism of Corynebacterium glutamicum by nuclear magnetic resonance spectroscopy combined with metabolite balancing.* Biotechnology and Bioengineering, 1996. **49**: p. 111-129.
25. Beyß, M., et al., *The design of FluxML: A universal modeling language for 13C metabolic flux analysis.* Frontiers in Microbiology, 2019. **10**.
26. Wiechert, W., et al., *A universal framework for 13C metabolic flux analysis.* Metabolic Engineering, 2001. **3**: p. 265-283.
27. Weitzel, M., *High Performance Algorithms for Metabolic Flux Analysis*. 2010. p. 319.
28. Lee, J.M., E.P. Gianchandani, and J.A. Papin, *Flux balance analysis in the era of metabolomics.* Briefings in Bioinformatics, 2006. **7**: p. 140-150.
29. Feist, A.M. and B.O. Palsson, *The biomass objective function.* Current Opinion in Microbiology, 2010. **13**: p. 344-349.
30. Gianchandani, E.P., A.K. Chavali, and J.A. Papin, *The application of flux balance analysis in systems biology.* Systems Biology and Medicine, 2010. **2**: p. 372-382.
31. Becker, S.A., et al., *Quantitative prediction of cellular metabolism with constraint-based models: the COBRA Toolbox.* Nature Protocols, 2007. **2**: p. 727-738.
32. Schellenberger, J., et al., *Quantitative prediction of cellular metabolism with constraint-based models: the COBRA Toolbox v2.0.* Nature Protocols, 2011. **6**: p. 1290-1307.
33. Nöh, K., et al., *Metabolic flux analysis at ultra short time scale: isotopically non-stationary 13C labeling experiments.* Journal of Biotechnology, 2007. **129**: p. 249-267.
34. Kjeldsen, K.R. and J. Nielsen, *In silico genome-scale reconstruction and validation of the Corynebacterium glutamicum metabolic network.* Biotechnology and Bioengineering, 2009. **102**: p. 583-597.
35. Becker, J., C. Klopprogge, and C. Wittmann, *Metabolic responses to pyruvate kinase deletion in lysine producing Corynebacterium glutamicum.* Microbial Cell Factories, 2008. **7**.
36. Bartek, T., et al., *Comparative 13C metabolic flux analysis of pyruvate dehydrogenase complex-deficient, L-valine-producing Corynebacterium glutamicum.* Applied and Environmental Microbiology, 2011. **77**: p. 6644-52.
37. Kind, S., J. Becker, and C. Wittmann, *Increased lysine production by flux coupling of the tricarboxylic acid cycle and the lysine biosynthetic pathway--metabolic engineering of the availability of succinyl-CoA in Corynebacterium glutamicum.* Metabolic Engineering, 2013. **15**: p. 184-95.
38. Wittmann, C. and E. Heinzle, *Genealogy Profiling through Strain Improvement by Using Metabolic Network Analysis : Metabolic Flux Genealogy of Several Generations of Lysine-Producing Corynebacteria.* Applied and Environmental Microbiology, 2002. **68**: p. 5843-5859.
39. Dekkers, J.G.J., H.E. de Kok, and J.A. Roels, *Energetics of Saccharomyces cerevisiae CBS426: Comparison of Anaerobic and Aerobic Glucose Limitation.* Biotechnology and Bioengineering, 1981. **23**: p. 1023-1035.
40. Kappelmann, J., W. Wiechert, and S. Noack, *Cutting the gordian knot: identifiability of anaplerotic reactions in Corynebacterium glutamicum by means of ^{13}C-metabolic flux analysis.* Biotechnology & bioengineering, 2016. **113**(3): p. 661 - 674.
41. Petersen, S., et al., *In Vivo Quantification of Parallel and Bidirectional Fluxes in the Anaplerosis of Corynebacterium glutamicum.* The Journal of Biological Chemistry, 2000. **275**: p. 35932-35941.

42. Zhao, Z., et al., *Substrate cycles in Penicillium chrysogenum quantified by isotopic non-stationary flux analysis.* Microbial Cell Factories, 2012. **11**: p. 140.
43. Cueto-Rojas, H.F., et al., *In vivo analysis of NH4+ transport and central N-metabolism of Saccharomyces cerevisiae under aerobic N-limited conditions.* Applied and environmental microbiology, 2016.
44. Liu, Y., et al., *A dynamic pathway analysis approach reveals a limiting futile cycle in N-acetylglucosamine overproducing Bacillus subtilis.* Nature Communications, 2016. **7**: p. 1-9.
45. Matsushita, K., et al., *NADH dehydrogenase of Corynebacterium glutamicum Purification of an NADH dehydrogenase II homolog able to oxidize NADPH.* FEMS Microbiology Letters, 2001. **204**: p. 271-276.
46. Nantapong, N., et al., *Electron transfer ability from NADH to menaquinone and from NADPH to oxygen of type II NADH dehydrogenase of Corynebacterium glutamicum.* Bioscience, Biotechnology, and Biochemistry, 2005. **69**: p. 149-159.
47. Dauner, M., T. Storni, and U. Sauer, *Bacillus subtilis Metabolism and Energetics in Carbon-Limited and Excess-Carbon Chemostat Culture.* Journal of Bacteriology, 2001. **183**: p. 7308-7317.
48. Limberg, M.H., et al., *Metabolic Profile of 1 , 5-Diaminopentane Producing Corynebacterium glutamicum Under Scale-Down Conditions : Blueprint for Robustness to Bioreactor Inhomogeneities.* Biotechnology and bioengineering, 2017. **114**: p. 560-575.
49. Käß, F., et al., *Rapid assessment of Oxygen Transfer Impact for Corynebacterium glutamicum.* Bioprocess and biosystems engineering, 2014. **37**(12): p. 2567 - 2577.
50. Käß, F., et al., *Assessment of robustness against dissolved oxygen/substrate oscillations for C. glutamicum DM1933 in two-compartment bioreactor.* Bioprocess and biosystems engineering, 2014. **37**: p. 1151-1162.
51. Limberg, M.H., et al., *Plug flow versus stirred tank reactor flow characteristics in two-compartment scale-down bioreactor: Setup-specific influence on the metabolic phenotype and bioprocess performance of Corynebacterium glutamicum.* Engineering in Life Sciences, 2016. **16**: p. 610-619.
52. Xu, B., et al., *Glucose overflow metabolism and mixed-acid fermentation in aerobic large-scale fed-batch processes with Escherichia coli.* Applied Microbiology and Biotechnology, 1999. **51**: p. 564-571.
53. Delvigne, F., J. Destain, and P. Thonart, *Bioreactor hydrodynamic effect on Escherichia coli physiology: experimental results and stochastic simulations.* Bioprocess and biosystems engineering, 2005. **28**: p. 131-137.
54. Hewitt, C.J., et al., *Studies related to the scale-up of high-cell-density E. coli fed-batch fermentations using multiparameter flow cytometry: effect of a changing microenvironment with respect to glucose and dissolved oxygen concentration.* Biotechnology and bioengineering, 2000. **70**: p. 381-390.
55. Moon, T.S., et al., *Production of glucaric acid from a synthetic pathway in recombinant Escherichia coli.* Applied and Environmental Microbiology, 2009. **75**: p. 589-595.
56. Soini, J., K. Ukkonen, and P. Neubauer, *High cell density media for Escherichia coli are generally designed for aerobic cultivations - consequences for large-scale bioprocesses and shake flask cultures.* Microbial Cell Factories, 2008. **7**.
57. Neubauer, P., L. Häggström, and S.O. Enfors, *Influence of substrate oscillations on acetate formation and growth yield in Escherichia coli glucose limited fed-batch cultivations.* Biotechnology and Bioengineering, 1995. **47**: p. 139-146.
58. Lejeune, A., F. Delvigne, and P. Thonart, *Influence of bioreactor hydraulic characteristics on a Saccharomyces cerevisiae fed-batch culture: hydrodynamic modelling and scale-down investigations.* Journal of industrial microbiology & biotechnology, 2010. **37**: p. 225-236.
59. George, S., G. Larsson, and S.O. Enfors, *A scale-down two-compartment reactor with controlled substrate oscillations: Metabolic response of Saccharomyces cerevisiae.* Bioprocess Engineering, 1993. **9**: p. 249-257.

60. Junne, S., et al., *A two-compartment bioreactor system made of commercial parts for bioprocess scale-down studies: impact of oscillations on Bacillus subtilis fed-batch cultivations.* Biotechnology Journal, 2011. **6**: p. 1009-1017.
61. Jensen, P.R. and O. Michelsen, *Carbon and energy metabolism of atp mutants of Escherichia coli.* Journal of Bacteriology, 1992. **174**: p. 7635-7641.
62. Santana, M., et al., *Bacillus subtilis FOF1 ATPase : DNA Sequence of the atp Operon and Characterization of atp Mutants.* 1994. **176**: p. 6802-6811.
63. Koul, A., et al., *Diarylquinolines are bactericidal for dormant mycobacteria as a result of disturbed ATP homeostasis.* The Journal of biological chemistry, 2008. **283**: p. 25273-80.
64. Koul, A., et al., *Diarylquinolines target subunit c of mycobacterial ATP synthase.* nature chemical biology, 2007. **3**: p. 323-324.
65. Tran, S.L. and G.M. Cook, *The F1Fo -ATP Synthase of Mycobacterium smegmatis Is Essential for Growth.* Journal of Bacteriology, 2005. **187**: p. 5023-5028.
66. Cook, G.M., et al., *Energetics of Respiration and Oxidative Phosphorylation in Mycobacteria.* Microbiology Spectrum, 2014: p. 1-20.